Two dimensional Cartesian airgap element (CAGE) for dynamic FE modeling of electrical machines with a flat airgap (repository copy)

Two-Dimensional Cartesian Air-Gap Element (CAGE) for Dynamic Finite Element Modeling of Electrical Machines With a Flat Air Gap

R. Wang, H. Mohellebi, T. J. Flack, M. J. Kamper, J. D. Buys, and M. Feliachi

Abstract— **This paper extends the air-gap element (AGE) to enable the modeling of flat air gaps. AGE is a macroelement originally proposed by Abdel-Razek *et al.* for modeling annular air gaps in electrical machines. The paper presents the theory of the new macroelement and explains its implementation within a time-stepped finite-element (FE) code. It validates the solution obtained by using an FE mesh with a discretized air gap. It then applies the model to determine the open-circuit electromotive force of an axial-flux permanent-magnet machine and compares the results with measurements.**

Index Terms— **Air gaps, finite-element methods, linear motors, magnetic fields, mesh generation, permanent magnet generators.**

I. Introduction

THE air-gap element (AGE) was originally proposed by Abdel-Razek et al. [1], [2] for the modeling of the annular air-gap region in electrical machines. The AGE replaces the finite-elements, which would normally be used to discretize the air-gap, with a single macro element. This macro-element is based on the analytical solution of the air-gap field. The main advantages of the AGE are: the ease with which relative motion between rotor and stator is treated (no need for re-meshing the air-gap); greater accuracy, since the air-gap field is related to its analytical solution; the avoidance of finite-elements with poor aspect ratios, or alternatively the use of a high peripheral density of nodes. The main disadvantage is that the resulting stiffness matrix has a large profile, especially if the number of nodes on the AGE boundary is large. This can lead to large CPU times, although a method for alleviating this problem is given in [3].

Since a typical rotating machine has an annular air-gap, the AGE was initially derived for the polar coordinate system. The modeling of some special electrical machines such as the linear machine or the disc-type rotating machine requires a basic reformulation of the AGE, in order to deal with the rectangular shape of the air-gap. Since this is associated with the Cartesian coordinate system it is necessary to derive the AGE for Cartesian problems. This paper presents the development of a Cartesian Air-Gap Element (CAGE). The new CAGE is validated by comparison with results obtained using the standard FE method, in which the air-gap is discretized. The application of the CAGE is also illustrated by a typical case study.

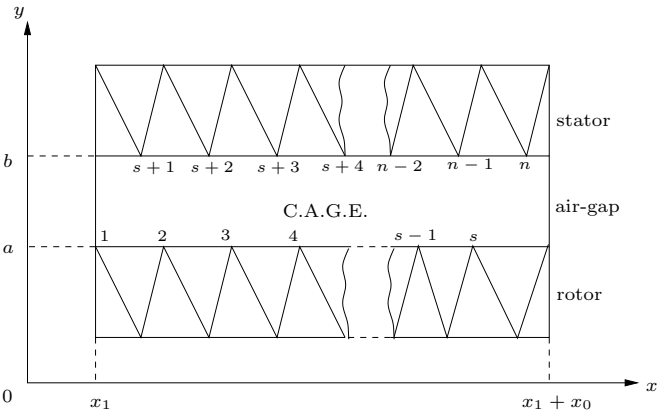

Fig. 1. Solution domain of the CAGE

II. Cartesian Air-Gap Element Model

Consider a generic linear machine, for which the air-gap is as shown in Fig. 1. Clearly, in the air-gap region there is no current, and the reluctivity is that of free space, ν_o. In Cartesian coordinates the field in the air-gap region is therefore governed by:

$$\frac{\partial^2 A(x,y)}{\partial x^2} + \frac{\partial^2 A(x,y)}{\partial y^2} = 0 \qquad (1)$$

in which $A(x,y)$ denotes the z-directed component of the magnetic vector potential. Like conventional electrical machines, special electrical machines such as the axial flux and the linear machine also exhibit structural periodicity which in turn leads to periodicity in the magnetic field distribution. In this paper the periodicity is taken to be of the form:

$$A(x,y) = A(x + x_o, y) \qquad (2)$$

Manuscript received February 1, 2001; revised October 17, 2001. This work was supported by the University of Stellenbosch, SA industry, and by THRIP funding

R. Wang and M. J. Kamper are with the Department of Electrical Engineering, University of Stellenbosch, Matieland 7602, South Africa (e-mail:rwang@ing.sun.ac.za; kamper@ing.sun.ac.za)

H. Mohellebi is with the Department of Electrotechnique, University of Mouloud MAMMERI, Tizi-Ouzou, BP17RP, Algeria (e-mail: mohellebi@yahoo.fr).

T. J. Flack is with the Engineering Department, Cambridge University, Cambridge CB2 1PZ, U.K. (e-mail: tjf@eng.cam.ac.uk).

J. D. Buys is with the Department of Mathematics, University of Stellenbosch, Matieland 7602, South Africa (e-mail: jdb@land.sun.ac.za).

M. Feliachi is with the GE44- (LRTI-IUT3), CRTT, Bd de l'Universit, BP406, 44602 Saint-Nazaire cedex, France (e-mail: moulond.feliachi@ge44.univ-nantes.fr).

where x_o is the period of the function $A(x,y)$. Applying the technique of separation of variables and applying the boundary condition of (2), the solution to (1) is

$$A(x,y) = F_o \cdot y + G_o + \sum_{n=1}^{\infty}(F_n \cdot e^{\lambda_n y} + G_n \cdot e^{-\lambda_n y}) \cdot (H_n \cos\lambda_n x + K_n \sin\lambda_n x). \quad (3)$$

where $\lambda_n = \pm 2n\pi/x_o$ and F_o, G_o, F_n, G_n, H_n, K_n are constants which are to be determined.

In order to maintain the continuity of A(x,y) at the transition between classical finite-elements and the CAGE (i.e. the lines $y = a$ and $y = b$), the following boundary condition must be satisfied:

$$A(x,c) = \sum_{i=k}^{l} \alpha_i(x,c) \cdot A_i^b \quad (4)$$

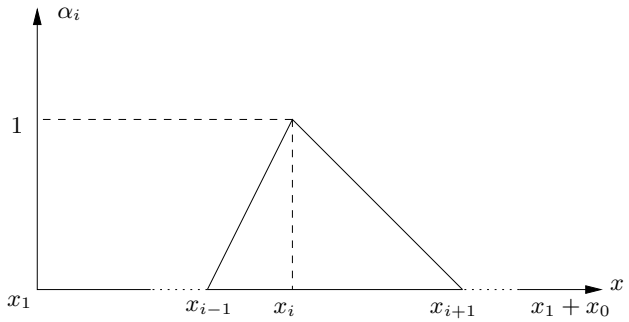

Fig. 2. Definition of function $\alpha_i(x,c)$

where A_i^b is the nodal value of the magnetic vector potential at node i on the CAGE boundary, $\alpha_i(x,c)$ is the Lagrange polynomial defined from the shape functions of the adjacent classical elements, and

$$k = \begin{cases} 1 & \text{and } l = s \text{ if } c = a, \\ s+1 & \text{and } l = t \text{ if } c = b. \end{cases}$$

The nodal shape function $\alpha_i(x,c)$ for the first order triangular element is illustrated in Fig. 2. This may be represented as:

$$\alpha_i(x,c) = \begin{cases} \frac{x - x_{i-1}}{x_i - x_{i-1}} & \text{if } x_{i-1} \le x \le x_i \\ \frac{x - x_{i+1}}{x_i - x_{i+1}} & \text{if } x_i \le x \le x_{i+1} \\ 0 & \text{if } x_1 \le x \le x_{i-1} \\ 0 & \text{if } x_{i+1} \le x \le x_1 + x_o \end{cases} \quad (5)$$

To facilitate further mathematical manipulation, Eq. (5) is expanded into a Fourier series:

$$\alpha_i(x,c) = a_{0i} + \sum_{n=1}^{\infty}[a_{ni}\cos\lambda_n x + b_{ni}\sin\lambda_n x] \quad (6)$$

where a_{0i}, a_{ni} and b_{ni} may be found as:

$$\begin{cases} a_{0i} = \frac{x_{i+1} - x_{i-1}}{x_o} \\ a_{ni} = -\frac{4}{x_o} \cdot \frac{1}{\lambda_n^2}\left[\frac{1}{x_i - x_{i-1}} \sin\frac{\lambda_n(x_i + x_{i-1})}{2} \sin\frac{\lambda_n(x_i - x_{i-1})}{2} + \frac{1}{x_i - x_{i+1}} \sin\frac{\lambda_n(x_{i+1} + x_i)}{2} \sin\frac{\lambda_n(x_{i+1} - x_i)}{2}\right] \\ b_{ni} = \frac{4}{x_o} \cdot \frac{1}{\lambda_n^2}\left[\frac{1}{x_i - x_{i-1}} \sin\frac{\lambda_n(x_i - x_{i-1})}{2} \cos\frac{\lambda_n(x_i + x_{i-1})}{2} + \frac{1}{x_i - x_{i+1}} \sin\frac{\lambda_n(x_{i+1} - x_i)}{2} \cos\frac{\lambda_n(x_{i+1} + x_i)}{2}\right] \end{cases} \quad (7)$$

The constants in Eq. (3) may now be found by equating $A(x,a)$ and $A(x,b)$ obtained from Eq. (3) with the respective terms obtained by substituting Eq. (6) into Eq. (4). The final result is:

$$A(x,y) = \sum_{i=1}^{t} \alpha_i^{\varepsilon}(x,y) \cdot A_i^b \quad (8)$$

where $\alpha_i^{\varepsilon}(x,c)$ is given by:

$$\alpha_i^{\varepsilon}(x,c) = \frac{y-c}{c'-c} \cdot \frac{a_{oi}}{2} + \sum_{n=1}^{\infty} \frac{e^{\lambda_n(y-c)} - e^{\lambda_n(c-y)}}{e^{\lambda_n(c'-c)} - e^{\lambda_n(c-c')}} \cdot (a_{ni}\cos\lambda_n x + b_{ni}\sin\lambda_n x). \quad (9)$$

and

$$c = \begin{cases} a \text{ and } c' = b \text{ if } i \in \{1,2,\ldots,s\} \\ b \text{ and } c' = a \text{ if } i \in \{s+1,\ldots,t\} \end{cases}$$

The energy functional for the air-gap, $[S]^{\varepsilon}$, is:

$$F_{\varepsilon} = \frac{1}{\mu_o}\int\int_{S_{\varepsilon}} \frac{B^2}{2} dS_{\varepsilon} \quad (10)$$

By substituting for B in Eq. (10) using $B = \nabla \times A$, where $A(x,y)$ is given by Eq. (8) and (9), and then differentiating with respect to A_i for $i = 1 \ldots t$ gives:

$$\frac{\partial F^{\varepsilon}}{\partial [A]^{\varepsilon}} = \frac{1}{\mu_o}[S]^{\varepsilon}[A]^{\varepsilon} \quad (11)$$

where the general term of the matrix $[S]^{\varepsilon}$ is:

$$\begin{aligned} S_{ij}^{\varepsilon} = {} & \frac{x_o}{4}\frac{b-a}{(c'-c)(f'-f)} a_{oi} a_{oj} \\ & + \frac{x_o}{2}\sum_{n=1}^{\infty} \frac{\lambda_n}{[e^{\lambda_n(c'-c)} - e^{\lambda_n(c-c')}]} \\ & \cdot \frac{1}{[e^{\lambda_n(f'-f)} - e^{\lambda_n(f-f')}]}[(e^{\lambda_n(b-c)} - e^{\lambda_n(c-b)}) \\ & \cdot (e^{\lambda_n(b-f)} + e^{\lambda_n(f-b)}) - (e^{\lambda_n(a-c)} - e^{\lambda_n(c-a)}) \\ & \cdot (e^{\lambda_n(a-f)} + e^{\lambda_n(f-a)})](a_{ni}a_{nj} + b_{ni}b_{nj}). \end{aligned} \quad (12)$$

where

$$f = \begin{cases} b \text{ and } f' = a \text{ if } i \in \{1,2,\ldots,s\} \\ a \text{ and } f' = b \text{ if } i \in \{s+1,\ldots,t\} \end{cases}$$

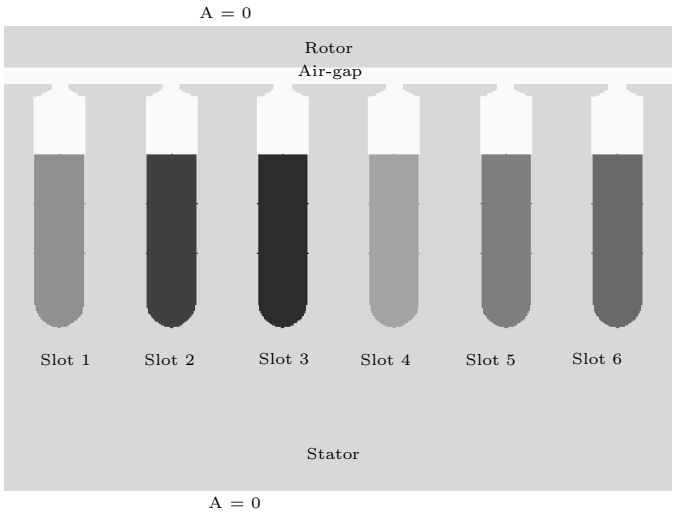

Fig. 3. Simple linear electrical machine model.

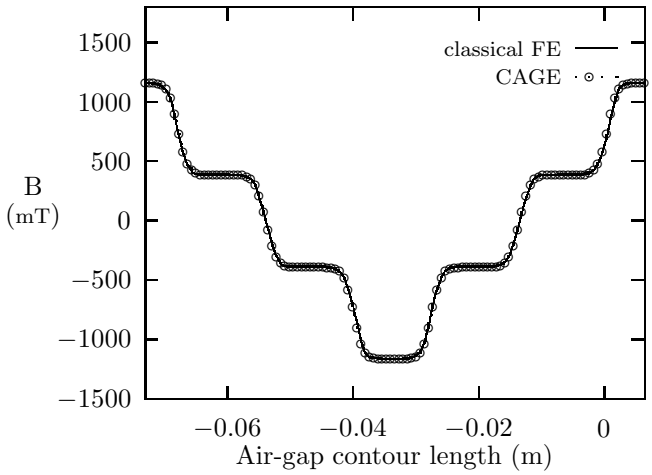

Fig. 4. Comparison of calculated air-gap flux density by using classical FE and C.A.G.E.

III. Coupling Scheme

The implementation of the CAGE into the standard finite element program is carried out in the same way as for the AGE for annular air-gaps. The energy-related functional is broken down into F^e and F^ε and is then minimized with respect to A:

$$\frac{\partial F}{\partial [A]} = \sum_{e=1}^{P} \frac{\partial F^e}{\partial [A]^e} + \frac{\partial F^\varepsilon}{\partial [A]^\varepsilon} \tag{13}$$

In order to reduce the time taken to compute the CAGE terms at different rotor positions, the scheme proposed in [3] was implemented. Close inspection of Eq. (12) and its counterpart for the annular AGE [1] reveals that this scheme can be directly applied to the CAGE with very little modification. In order to further reduce the CPU time taken, it was possible to utilize a negative periodic model, thus reducing the number of unknowns to be solved for by a factor of two approximately. The modification to the CAGE for negative periodic boundary conditions was done in the same manner proposed in [3], which proves that the first term in Eq. (12) disappears, and the second term is doubled.

IV. Validation by Comparison

In order to validate the CAGE, the simplified linear problem shown in Fig. 3 was modeled. Firstly the air-gap was discretized using two layers (120 nodes per layer) of classical first-order triangular elements, and the resulting FE model solved. Then, the CAGE was substituted in place of the discretized air-gap, leaving the rest of the FE mesh unchanged, and solved. Homogeneous Dirichlet conditions were assigned to the top and bottom boundaries, whilst positive periodicity conditions were assigned to the left and right boundaries.

Slots 1 - 6 were excited with balanced three-phase currents at an instant in time, and the air-gap flux density distribution obtained by both methods is plotted in Fig. 4. It is evident that the result obtained using the CAGE agrees very well with that obtained using a discretized air-gap.

Further examination and verification has also been performed by comparing the respective magnetic stored energies in various parts of the model obtained from both methods, as shown in Table 1. It is evident that the results are in very good agreement. The worst discrepancy is about 0.5%.

V. Application

The 2D FE modeling of an iron-less stator AFPM machine [4] (illustrated in Fig. 5) is usually carried out by introducing a radial cutting plane, which is then developed

TABLE I
COMPARISON OF THE CALCULATED MAGNETIC STORED ENERGY IN DIFFERENT SUB-REGIONS OF THE MODEL

Regions	C.A.G.E. (μJ)	Classical FE (μJ)	Diff%
Slot1 (Cu)	0.519085776	0.519129716	0.01%
(air)	0.692833408	0.695610829	0.40%
Slot2 (Cu)	2.07633383	2.07650904	0.01%
(air)	2.69936816	2.69670033	0.09%
Slot3 (Cu)	0.519085782	0.519129719	0.01%
(air)	0.692830925	0.699608371	0.09%
Slot4 (Cu)	0.519085777	0.519129716	0.01%
(air)	0.692833425	0.699610829	0.09%
Slot5 (Cu)	2.07633377	2.07650904	0.01%
(air)	2.69936826	2.69670033	0.09%
Slot6 (Cu)	0.519085774	0.519129719	0.01%
(air)	0.692830919	0.695608317	0.40%
Stator iron	0.242891804	0.242665537	0.14%
Rotor iron	0.025792278	0.0254261082	0.14%
Air-gap	35.8157674	35.9925716	0.49%

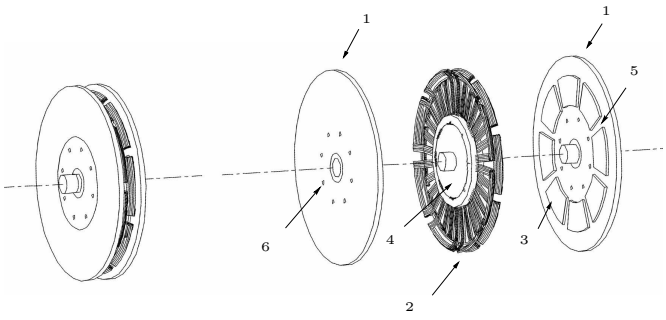

Fig. 5. Exploded view of an AFPM machine, 1 – rotor discs, 2 – stator winding, 3 – permanent magnets, 4 – epoxy core, 5 – radial channels, 6 – air-inlet holes.

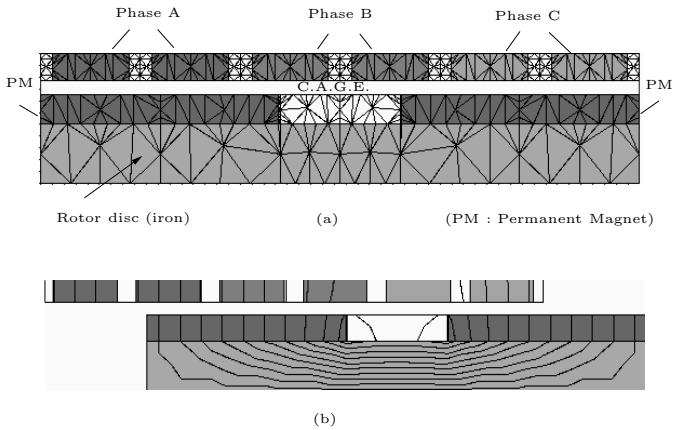

Fig. 6. Time-step FE model of an iron-less stator AFPM machine

into a 2D flat model. Figure 6(a) shows an FE mesh for such a model, which spans one pole of the AFPM machine. The mesh consists of 622 elements and 447 nodes (of which 138 nodes lie on the boundaries of the CAGE). The air-gap region was modeled using the CAGE. The model was time-stepped over a time interval of 16 ms (which corresponds to the rotor moving by one pole-pair), using a time-step of 0.2 ms. This required 80 FE solutions. Figure 6(b) shows the flux plot of the AFPM machine at a certain position. At every rotor position, the total phase flux linkages were determined from the FE field solution, from which the phase EMF $e(t)$ could be found as:

$$e(t) = \frac{d\lambda}{dt} = \frac{\lambda(\theta_2) - \lambda(\theta_1)}{t_2 - t_1} \tag{14}$$

The total CPU time for this simulation was 107 seconds on a 333 MHz PC running the Redhat Linux operating system. The calculated EMF induced in the stator phase winding at a shaft speed 970 rpm is compared with measurement in Fig. 7. It is seen that the correlation between calculated and measured EMF is very good.

VI. Conclusion

This paper has reported the development of a 2D CAGE, and validated it by comparison with the standard FE method. It has also shown that the CAGE is still a viable method for time-stepped FE modeling of electrical machines, and the method has been successfully applied to an AFPM machine. Measured and simulated results of the AFPM machine open-circuit EMF when driven at fixed speed were found to be in very good agreement. The CAGE formulation derived here is applicable to most linear machines and some other special machines such as rotating disc machines.

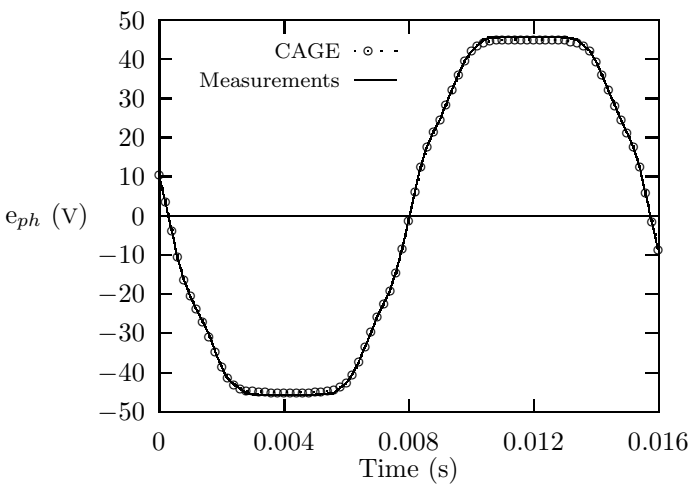

Fig. 7. Phase EMF as a function of time at 970 rpm

References

[1] A. A. Abdel-Razek, J. L. Coulomb, M. Feliachi, and J. C. Sabonnadiere, "The calculation of electromagnetic torque in saturated electric machines within combined numerical and analytical solution in the field equations", *IEEE Trans. Magn.*, vol. 17, no. 6, pp. 3250-3252, 1981.

[2] ——,"Conception of an air-gap element for the dynamic analysis of the electromagnetic field in electric machines", *IEEE Trans. Magn.* , vol. 18, no. 2, pp. 655-659, 1982.

[3] T. J. Flack and A. F. Volschenk, "Computational aspects of time-stepping finite-element analysis using an air-gap element", *Proceeding of International Conference on Electrical Machines*, Paris, 1994.

[4] N. F. Lombard and M. J. Kamper, "Analysis and Performance of an Iron-less Stator Axial Flux Permanent Magnet Machine," *IEEE Trans. Energy Conversion* , vol. 14, no. 4, pp.1051–1056, 1999.